

Dynamics and Cooperativity of Microtubule Decoration by the Motor Protein Kinesin

To appear in the Journal of Molecular Biology

Andrej Vilfan^{1,2}, Erwin Frey^{3,4}, Franz Schwabl¹

¹*Institut für Theoretische Physik, Technische Universität München
James-Franck-Strasse, 85747 Garching, Germany*

²*Cavendish Laboratory, Madingley Road, Cambridge CB3 0HE, UK*

³*Abteilung Theorie, Hahn-Meitner-Institut, Glienicker Strasse 100, 14109 Berlin, Germany*

⁴*Freie Universität Berlin, Fachbereich Physik, Arnimallee 14, 14195 Berlin, Germany*

Manfred Thormählen, Young-Hwa Song, Eckhard Mandelkow

Max-Planck-Unit for Structural Molecular Biology

Notkestrasse 85, 22607 Hamburg, Germany

Running title: Dynamics and cooperativity in kinesin-microtubule interactions

Keywords: molecular motors; tubulin; nucleation; annealing

Abbreviations: MAPs = microtubule-associated proteins; NCD = product of the non claret disjunctional gene

ABSTRACT

We describe a theoretical and experimental analysis of the interaction between microtubules and dimeric motor proteins (kinesin, NCD), with special emphasis on the stoichiometry of the interaction, cooperative effects, and their consequences for the interpretation of biochemical and image reconstruction results. Monomeric motors can bind equivalently to microtubules without interference, at a stoichiometry of one motor head per tubulin subunit ($\alpha\beta$ -heterodimer). By contrast, dimeric motors can interact with stoichiometries ranging between one and two heads per tubulin subunit, depending on binding constants of the first head and the subsequent binding of the second head, and the concentration of dimers in solution. Further we show that an attractive interaction between the bound motor molecules can explain the higher periodicities observed in decorated microtubules (e.g. 16 nm periodicity), and the non-uniform decoration of a population of microtubules and give an estimate on the strength of this interaction.

INTRODUCTION

Intracellular traffic of vesicles and organelles is largely the result of motor proteins moving along microtubules. Because of its fundamental importance, microtubule-dependent motility has been studied intensely by cell biologists and biophysicists. Most of these studies focus on motors from the kinesin superfamily such as kinesin or NCD. While a single dimeric kinesin molecule is able to move processively along a microtubule, a larger group of NCD or single-headed kinesin molecules is needed to transport a cargo^{1,2}. Although single motors can be observed in action with optical tweezers^{3,4} and modern light microscopy techniques^{5,6}, the structure of motors interacting with microtubules can be approached only by electron microscopy and averaging over many units by image processing methods. This explains the interest in microtubules fully "decorated" with motors. Several such studies have been reported and interpreted in terms of models of kinesin or NCD movement^{7,8,9,10,11,12}. Recently, the high-resolution structures of two key molecules (kinesin^{13,14,15,16,17} and tubulin^{18,19}) have been solved by diffraction methods, and low-resolution maps of microtubules decorated with motor proteins have been obtained by cryo-electron microscopy and image reconstruction^{7,8,9,10,11,12,20,21}. When combining these data with micromechanical^{4,22} and biochemical results one hopes to obtain a detailed view of the mechanochemistry of motors moving along a microtubule lattice. This goal has not yet been reached, partly because of limited resolution, disorder in the molecules, and ambiguities in the reported microtubule-motors interactions, such as the stoichiometries, the effects of nucleotides, or conformational changes of motors on the microtubule surface (reviewed by Mandelkow & Hoenger²³).

The interaction of large supramolecular biological polymers with protein ligands has been the topic of many experimental and theoretical studies (e.g. DNA-protein, virus-antibody, muscle actin-myosin). However, the motor-microtubule interaction presents some unique features: microtubules can be considered as a two-dimensional lattice of subunits, constrained to the surface of a cylinder. They contain two similar subunits (α - and β -tubulin) which occur as heterodimers, but only one of these (β -tubulin) is considered the main interaction partner of kinesin motors. Thus, the possible interaction sites for motors are spaced 8 nm longitudinally and 5 nm laterally on a microtubule surface, i.e. the tubulin-heterodimer is the effective "subunit" on the microtubule lattice (Fig. 2). The structure of tubulin has been solved by electron crystallography so that a high resolution model of the microtubule is available^{18,19}. Most motors also occur as dimers containing two motor domains with associated light chains^{24,25}. In contrast to tubulin, both motor heads of kinesin can serve as interaction partners. A motor complex can be bound to a microtubule either with both heads (on different tubulin subunits) or with only one head and the second head loosely tethered to the first one. These two possibilities are consistent with structural data²³ as well as with biochemical evidence (e.g. the non-equivalence of nucleotide exchange²⁶). The structures of kinesin and NCD in monomeric and dimeric states have been solved^{13,14,15,16,17} (reviewed by Sack et al.²⁷). One important result is that the structure of "free" motors (i.e. not bound to microtubules) would not fit onto a microtubule surface; the two heads do not have the proper orientation, and they are packed so tightly that they could not reach across two neighboring tubulin subunits. From these considerations it is clear that there must be major conformational changes when motors bind to microtubules. Two basic models have been put forward for the association of dimeric motors with microtubules, with predicted stoichiometries of 1 and 2, respectively. In the A-B model, the two heads of a dimer are largely independent of each other and bind to distinct neighboring tubulin subunits so that each tubulin subunit binds only one head ($n=1$). This mode is reminiscent of the binding of monomeric motor heads whose α -helical coiled coil domain is too short to support the dimeric state (see Fig. 2b). This model was proposed for rat brain kinesin²⁰. In the A^B model, one head of a dimeric motor binds directly and strongly to the microtubule surface, the second head is tethered to the first, so that effectively each tubulin subunit has two motor heads bound ($n=2$). This situation was experimentally observed with *Drosophila* NCD¹², and similar interpretations have been given for different forms of kinesin^{9,7,8}. Direct determinations of the binding stoichiometry of kinesin by biochemical assays and STEM indicated a stoichiometry of ~ 1 , compatible with the A-B model²⁸.

On the other hand, values higher than 1 were also observed, both for kinesin and NCD^{29,28}, and although some of the variance could be due to experimental error there was the possibility that this was due to some more fundamental problem²⁰. The idealized models, A-B and A^B leave out essential physics. They do not take into account that both states (A-B and A^B) can actually coexist on the lattice. Transitions between them depend on the binding kinetics of the first and the second head, but also on the crowding of the lattice. For example, steric constraints allow only the A^B state but not A-B state if both neighbouring sites are occupied with other dimers. For monomeric motors this issue is unimportant since we may assume that the binding sites on the microtubule are far apart, compared with the size of the motor domain. For dimeric motors the problem requires a more detailed analysis, as described below. The theoretical considerations predict that truly periodic binding of kinesin dimers in the A-B mode is possible only in special circumstances, requiring certain relationships between the rates of association and dissociation. Depending on the rate constants the average stoichiometries may have values anywhere between 1 and 2.

There are several experimental observations on decorated microtubules which can only be explained if in addition to the reaction kinetics of kinesin dimers and the crowding effects one takes into account an interaction between attached kinesin molecules. The first such observation is the two-dimensional ordering of kinesin dimers on microtubules which results in a longitudinal superperiodicity of 16 nm, twice the spacing of tubulin subunits along the protofilaments²⁸, laterally in phase. We shall show that this phenomenon can be explained by an attractive interaction between kinesin dimers which leads to a state with higher order periodicity, either directly through single-site nucleation or gradually through annealing on the microtubule surface. Secondly, under certain conditions (e.g. substoichiometric ratios of kinesin to tubulin) we observe a clear phase separation between empty and decorated microtubules, to the extent that a single microtubule may be fully decorated in a neighborhood of empty microtubules. A similar observation has been reported for the substoichiometric decoration of myosin on actin filaments³⁰ and is another strong indication for a cooperative element in the kinesin-microtubule interaction, akin to the aggregation of adsorbed layers on crystal surfaces. The cooperativity could be mediated either by direct interactions between bound kinesin molecules, or indirectly through the microtubule lattice which may act as a sensor for incoming motor molecules.

One should also note that the decoration process of an initially empty microtubule surface is a quite complex dynamic process. There are several dynamic regimes. Initially, kinesin dimers are decorating the surface in a random fashion, leaving unoccupied holes. The holes are generated because of the crowding effect discussed above. Annealing into a perfectly periodic structure occurs in a second phase which requires the transient dissociation and reshuffling of motor heads. Since this process is expected to be very slow, we suggest that the periodic structure can be reached much faster via single-site nucleation.

The purpose of this article is twofold. We study theoretically the binding of dimeric kinesin-like proteins on microtubules and also present new experimental results showing cooperative decoration. Along with stoichiometry measurements and the observation of two-dimensional ordering, this is the third major observation our theory is based on. In the theoretical model we assume that kinesin can either bind to a single site on the lattice with one of its heads or with both heads to adjacent sites of the same protofilament. In the first part, we study the model without any interaction between kinesin molecules (besides the fact that only one head can bind to a binding site), which is fully analytically solvable. This allows us to provide a quantitative analysis of decoration experiments and to give an explanation for seemingly contradictory experimental results, which have been a matter of controversy over the last years^{29,28}. Later on we introduce an attraction between adsorbed kinesin molecules. We give an estimate on how strong this interaction has to be in order to explain the observed 16nm periodicity and the coexistence of empty and decorated domains. We finally discuss in detail the implications of our theory.

RESULTS

1. Decoration of microtubules by kinesin: Experimental evidence for cooperative effects

In electron microscopic images of negatively stained microtubule preparations there are two prominent features: protofilaments axially spaced at 5 nm intervals, and the tubulin monomers (α or β) that make up the protofilaments and give rise to a 4 nm longitudinal periodicity. Due to the high structural similarity of α - and β -tubulin, the signal that arises from the 8 nm periodicity of $\alpha\beta$ -tubulin heterodimers is usually very small²⁸.

As kinesin motor domains have only one tight binding site per $\alpha\beta$ -tubulin-dimer, the full decoration of microtubules by kinesin monomers enhances the 8 nm longitudinal contrast variations and reveals the 10° inclination of the 3-start helix which is the hallmark of the B-lattice of tubulin dimers³¹. The signature of a decorated microtubule wall is the 8 nm periodicity resulting from regular kinesin binding²⁸. Here, microtubules have been saturated by the monomeric kinesin construct sqK338 which lacks the entire dimerization domain. In most cases, microtubules decorated with dimeric constructs, i.e. constructs that form coiled-coils due to heptad repeats in their neck and stalk regions (such as sqK498) will give a similar picture. However, sometimes an additional feature can be recognized, namely a longitudinal periodicity spaced at 16 nm intervals. In the case of decorated tubulin sheets this was interpreted as two kinesin heads bound to successive tubulin dimers and joined together via their coiled-coil neck and stalk³². In rare cases the same phenomenon can also be observed on cylindrical microtubules (Figure 1a). If the paired kinesin heads are aligned in register on adjacent protofilaments (i.e. parallel to the 3-start helix) this will generate a 16 nm modulation of the striations running across the microtubule lattice. On the other hand, if the kinesin dimers were completely free to attach to adjacent protofilaments either in register or out of register the 16 nm periodicity would be averaged out. We therefore conclude that there must be a mechanism which allows an approaching kinesin dimer to sense the presence of an adjacent bound dimer on a neighboring protofilament and attach to the microtubule in an ordered and cooperative fashion. Conversely, the 16 nm periodicity is not observed with monomeric kinesin constructs, confirming that the crosstalk between kinesin-dimers on the microtubule surface is the basis of the effect.

In most experiments full decoration is brought about by using a more than stoichiometric ratio of kinesin to tubulin. To obtain a better understanding of the mechanisms responsible for ordered kinesin binding, we performed experiments in which the ratio of kinesin to tubulin was less than stoichiometric (experimental ratios nominally ranged from three to one tubulin dimers per kinesin motor domain). Under these conditions two possible results were predicted. Kinesin could bind stochastically, thus eliminating the pronounced decoration effect. Alternatively, kinesin could bind in a cooperative fashion leading to areas on microtubules showing a high level of decoration, and other areas with low or no decoration. In the extreme case, one microtubule could be fully decorated while others are bare. The latter situation is indeed observed; Fig. 1b shows a field of microtubules decorated with the dimeric construct rK379 at a nominal stoichiometry of 1 motor domain per tubulin subunit. Two microtubules show the 8 nm periodicity and jagged edges characteristic of kinesin decoration, while one shows no 8 nm periodicity and has smooth edges, it does not seem to be decorated at all. This behavior indicates a high level of cooperativity between individual kinesin dimers. As in the case of the 16 nm periodicities, the effect is only observed with dimeric kinesin constructs. The dimeric construct sqK411 at ratios between 1 : 1 and 1 : 3 (motor domain : tubulin dimer) yielded results identical to those presented here. However, the monomeric construct rK354 showed no clear decoration under the same conditions. This behavior is reminiscent of a similar selective decoration process observed for actin filaments decorated with dimeric myosin (heavy meromyosin fragment, HMM) at low stoichiometries, but not with monomeric myosin subfragment-1 (S-1)³⁰.

In the following sections we present our efforts to analytically describe the dynamics of decoration and simulate it by computer modeling. We show that the binding stoichiometries as well as cooperative phenomena can be described by a simple basic model with few adjustable parameters. Moreover, the model shows that the effective stoichiometry of kinesin-tubulin binding can vary continuously, depending on the kinetic parameters of decoration and kinesin concentration.

2. Microtubule decoration by kinesin monomers and dimers (non-interacting)

The theoretical model describes the experimental situation found in a typical decoration assay. It starts with an empty microtubule lattice surrounded by a solution of single- or double-headed kinesin molecules (Fig. 2a, b). In the case of *monomeric* kinesin constructs, each kinesin can attach to a binding site on β -tubulin independently of its neighbors. The binding sites on the microtubule are far apart, compared to the size of the kinesin head, and therefore the problem of steric overlap does not occur, nor do the kinesin molecules interact cooperatively, in agreement with the experimental results (Fig. 2a). The association and dissociation rates of the kinesin heads to microtubules have been determined by several groups^{26,33,34} (reviewed by Mandelkow & Johnson³⁵). The values in the presence of ADP and low salt concentration are approximately $k_{+1}=10 \mu\text{M}^{-1}\text{s}^{-1}$ and $k_{-1}=10 \text{s}^{-1}$. These values give the binding constant $K_1 = k_{+1}/k_{-1} = 1\mu\text{M}^{-1}$ and the binding stoichiometry v given by Langmuir's isotherm

$$v = \frac{K_1 c}{1 + K_1 c}, \quad (1)$$

where c denotes the solution concentration of kinesin monomers.

Next we turn to the case of decoration by *dimeric* kinesin (Fig. 2b). The kinesin dimers can either attach with one head onto a binding site on β -tubulin (state B^A or A^B) or with two heads on two adjacent binding sites on a protofilament (state A-B). The attached heads can also detach at some rate. As with kinesin monomers, we assume for the moment that there is no interaction between attached kinesin dimers except for steric reasons, i.e. two heads cannot attach to the same binding site at a time. This means that – to a first approximation - kinesin dimers attached to different protofilaments do not influence each other. Each protofilament can be described independently and we can simplify it to a one-dimensional model. In the model a dimer can bind with one head to each free site of the one-dimensional lattice. The binding rate ($k_{+1}c$) is proportional to the kinesin concentration. Since the linkage between the two heads is flexible, binding of both heads occurs consecutively. This is consistent both with the biochemical evidence²⁶ and with image reconstruction analysis suggesting that kinesin heads must open up in their neck region when binding to a microtubule¹¹. We neglect any influence the second (not yet bound) head could have on the binding rate of the first one.

After docking of the first head, the second head of a dimer can bind to an empty site either in front of or behind the first one (to state A-B). The corresponding probabilities (k_{+2}^f, k_{+2}^b , Fig. 3a) might be different since kinesin heads and microtubules are polar structures. A dimer with both heads attached to different microtubule subunits can detach one of its heads (from state A-B to state B^A or A^B). Again, the probabilities for the detachment of the front (k_{-2}^f) and the rear head (k_{-2}^b) can be different. A dimer attached with only one head can detach from the lattice completely (k_{-1}). These reactions are summarized in Fig. 3a. Since we are only interested in modeling the decoration and not in motility we consider a situation in which there is no ATP hydrolysis upon kinesin binding (i.e. the solution may contain AMP-PNP, ADP, or no nucleotide). Then there is no energy source in the system, and the reaction rates obey *detailed balance*, which states that the ratio between the forward and backward reaction rate depends only on the difference in free energy, which is the same if the front or the rear head detaches. This leads to a constraint on the reaction rates:

$$\frac{k_{+2}^b}{k_{-2}^b} = \frac{k_{+2}^f}{k_{-2}^f} = K_2. \quad (2)$$

Eq. (2) remains valid even if the front and the rear head bind different nucleotides (e.g. front head without a nucleotide, rear head with AMP-PNP). The major quantity of interest is the binding stoichiometry, giving the number of attached kinesin heads per tubulin binding site as a function of kinesin concentration. Generally, the kinesin-microtubule decoration model (neglecting for the moment any interactions between kinesin molecules) is described by five independent reaction rates (Fig. 4). However, the equilibrium binding stoichiometry depends only on the solution concentration c and the free energy difference between the states, which is expressed in the reaction constants (K_1 and K_2). They are characteristic for the particular type of motor protein (different kinds of kinesin or NCD) and the nucleotide bound to it (ADP, AMP-PNP etc.). At low concentrations, where the attached molecules do not interfere with each other, they can be written as

$$K_1 = \frac{[\text{Kin. bound on one head}] \times [\text{Kin. in solution}]}{[\text{Tubulin}]}, \quad (3)$$

$$K_2 = \frac{[\text{Kin. bound on both heads}]}{[\text{Kin. bound on one head}]}.$$

To estimate their values, we again use data measured by Moyer et al.³⁴ in the presence of ADP and low salt concentration: $k_{+1}=20 \mu\text{M}^{-1}\text{s}^{-1}$ and $k_{-1}=25 \text{s}^{-1}$, leading to $K_1=0.8 \mu\text{M}^{-1}$. Determining the binding constant from experiments measuring the reaction kinetics is more difficult since transitions occur in different nucleotide states. An estimate for the binding and unbinding rates of the second head³⁴ gives $k_{+2}=300 \text{s}^{-1}$ and $k_{-2}=50 \text{s}^{-1}$ and thus $K_2=6.0$. This is just a rough estimate since we have not considered the difference between k_{+2}^b and k_{+2}^f (or the reverse rates), the nature of the bound nucleotide (binding is stronger with AMP-PNP than with ADP) and the ionic strength. Another estimate of the constant K_2 is possible from comparison of the detachment times for single- and double-headed kinesin, measured by Hancock and Howard³⁶. If one assumes that the binding and unbinding constants for the first head of a dimer are the same as those for a monomer and that the second head equilibrates sufficiently fast, the slowing-down of the detachment rate becomes $k_{-}^{\text{Dimer}} : k_{-}^{\text{Monomer}} = 1 : (K_2 + 1)$. The measurements suggest $K_2 \approx 2.7$ in the presence of ADP, $K_2 \approx 8$ in the presence of AMP-PNP and $K_2 \approx 20$ without a nucleotide. Of course, our theory is not limited to a given set of parameters. If the stoichiometry data are known with sufficient accuracy, it may even be used to extract the binding constants from experimental data. Aided by our theoretical analysis one could in principle use stoichiometry measurements as a method to determine the influence of different chemical conditions or mutations on the binding constants of the first and the second head.

(a) Equilibrium stoichiometry

To determine the equilibrium configuration of our dimer adsorption model, we use a description as shown in Fig. 3b. "D" represents a dimer tightly bound with both heads to two different β -tubulin subunits, "1" represents a kinesin dimer bound through one head only (the other one being loosely tethered), and "0" represents an empty binding site. Since there is no interaction between the elements, the probability to find a certain sequence with elements "0", "1" and "D" has to be invariant against permutations of the elements. We denote the probability to find an empty site at a given place in the sequence as p_0 , to find a dimer attached with one head as p_1 and to find a dimer attached with both heads as p_D . The normalization reads $p_0 + p_1 + p_D = 1$. If we now observe a large sequence of N elements the probability to find the configuration (e_1, e_2, \dots, e_N) will be $p_{e_1} p_{e_2} \dots p_{e_N}$, where e_i can have values "0", "1" or "D". It will on average contain $N p_0$ empty sites, $N p_1$ single-bonded dimers and $N p_D$ double bonded dimers and will occupy $N(p_0 + p_1 + 2 p_D)$ binding sites on the tubulin lattice.

The principle of detailed balance states that for each pair of possible configurations, their probabilities are in the same ratio as the transition rates between these two configurations. The transitions between the configuration $(e_1, \dots, 0, \dots, e_N)$ and $(e_1, \dots, 1, \dots, e_N)$ occur with rates $k_{+1}c$ and k_{-1} , and the probabilities of these configurations are $p_{e_1} \dots p_0 \dots p_{e_N}$ and $p_{e_1} \dots p_1 \dots p_{e_N}$. This means that the ratio between the probabilities for both configurations is

$$\frac{p_1}{p_0} = \frac{k_{+1}c}{k_{-1}} = K_1 c. \quad (4)$$

The transitions connected with the binding of the second head are analog. The transition rates between the states $(e_1, \dots, 1, 0, \dots, e_N)$ and $(e_1, \dots, D, \dots, e_N)$ are k_{+2}^f and k_{-2}^f and their probabilities $p_{e_1} \dots p_1 p_0 \dots p_{e_N}$ and $p_{e_1} \dots p_D \dots p_{e_N}$. Thus detailed balance states

$$\frac{p_D}{p_0 p_1} = \frac{k_{+2}^{b,f}}{k_{-2}^{b,f}} = K_2. \quad (5)$$

These two equations, together with the normalization condition, uniquely determine the values p_0 , p_1 and p_D . The stoichiometry, i.e. the total number of heads per binding site can be calculated as twice the average number of bound dimers $N(p_1 + p_D)$, divided through the total number of binding sites $N(p_0 + p_1 + 2 p_D)$

$$v = 2 \frac{p_1 + p_D}{p_0 + p_1 + 2 p_D} = 1 + \frac{K_1 c - 1}{\sqrt{4 K_1 K_2 c + (1 + K_1 c)^2}}. \quad (6)$$

The number of bound heads whose partners are bound too is then given as

$$v_D = \frac{2 p_D}{p_0 + p_1 + 2 p_D} = 1 - \frac{K_1 c + 1}{\sqrt{4 K_1 K_2 c + (1 + K_1 c)^2}}. \quad (7)$$

It reaches its maximum for $c = 1/K_1$

$$v_D^{\max} \approx v_D(K_1 c = 1) = 1 - \frac{1}{\sqrt{K_2 + 1}}. \quad (8)$$

At this concentration the total stoichiometry is always $v=1$ (see Eq. (6)). In the limit $c \rightarrow \infty$ Eq. (6) yields $v=2$. Note that this does not mean that the stoichiometry 2 can always be reached in a real system. As can be inferred from Fig. 4a the limiting value 2 is approached only slowly with increasing concentration c . In an actual system such large values of c may, however, not be accessible. Besides the stoichiometry of all bound heads v Fig. 4a also shows the stoichiometry v_D of those heads belonging to doubly-bound dimers as a function of kinesin concentration c . A rough estimate with parameter values mentioned above ($K_1=0.8 \mu\text{M}^{-1}$, $K_2=6.0$) gives a stoichiometry of

$v=0.96$ at $1\mu\text{M}$ kinesin and $v=1.42$ at $10\mu\text{M}$. On the other hand, if we set $K_2=0$ as we expect for NCD, we obtain $v=0.89$ at $1\mu\text{M}$ and $v=1.82$ at $10\mu\text{M}$. The usage of these examples however, does not mean that the theory is limited to their values. Since the number of free parameters is only two, they could be well determined from a sufficiently accurate stoichiometry curve (which is unfortunately not yet available at present). Therefore Eq. (6) could be used to study the influence of different factors on binding constants. Any deviation from the symmetric form resulting from (6), on the other hand, indicates an additional interaction between dimers, which will be discussed in the next section.

Figure 4b shows the stoichiometry curves in a *Scatchard plot*, with the abscissa showing the average number of bound ligands per lattice site (in our case v) and the ordinate the same number divided through the solution concentration (v/c). Since models with fully independent ligands always show a linear dependence, any curvature indicates either that each ligand covers more than one binding site or that there is some cooperativity (attractive or repulsive) between the bound ligands^{37,38}. We obtain a linear curve for $K_2 = 0$ and a convex curve otherwise.

3. Decoration of microtubules with interactions between kinesin molecules

(a) Modeling of interactions between kinesin molecules on the microtubule surface

Thus far we have assumed that there is no interaction between attached dimers, except for the fact that each binding site can be occupied at most by one head. However, as mentioned above (Fig. 1), there is strong experimental evidence for the existence of an attractive interaction. Observations of two-dimensional crystalline ordering of kinesin dimers (e.g. 16 nm repeats) could not be explained without their lateral interaction across protofilaments. The coexistence of decorated and undecorated domains on microtubules further implies the existence of cooperative interactions.

We model this interaction as follows (Fig. 5): The presence of a kinesin head on the neighboring protofilament which acts attractively changes the attachment and the detachment rate of the observed head by factors A and B such that

$$\begin{aligned} k_{+1,+2}^{\text{with neighbor}} &= A_i k_{+1,+2}^{\text{without neighbor}} \\ k_{-1,-2}^{\text{with neighbor}} &= B_i k_{-1,-2}^{\text{without neighbor}} \end{aligned} \quad (10)$$

From detailed balance we get

$$J_i = k_B T \ln \frac{A_i}{B_i}, \quad (11)$$

where J_i denotes the interaction potential between two bound dimers. A_i , B_i and J_i may be different for different relative positions of the two heads, such as longitudinal (situation (I) in Fig. 5a), transverse between two dimers in register (situation II), transverse between a dimer with one attached head and one with two (situation III) etc. . In subsequent calculations we will assume that the interaction influences the attachment rate by the same factor as the detachment rate, thus $A_i=1/B_i$.

Even when assuming only nearest neighbor interaction, a general description would require 12 different constants characterizing the interaction strength between different states in different relative positions. Assuming a lateral symmetry (and therefore neglecting the fact that the tubulin lattice is not orthogonal) reduces their number to 9. Since these are still too many parameters for a general treatment, we use a simplified model by introducing only two different interaction constants, a longitudinal and a transverse one (Fig. 5a). This simplified description turns out to be sufficient to explain the essential experimental observations such as two-dimensional ordering and

segregation of decorated and empty domains. The longitudinal interaction constant is denoted by J_L and acts always between two heads on neighboring sites of the same protofilament. The transverse interaction has the strength J_T and acts between two heads attached on neighboring sites of two protofilaments. Since the model has to explain the experimentally observed lateral ordering²⁸, binding of a dimer out-of-phase with the decoration on the neighboring protofilament (Fig. 5a, IV) should be energetically less favored than binding in-phase (Fig. 5a, III). In terms of our simplified description, we assume the interaction between two staggered dimers, i.e. attached to adjacent protofilaments and shifted by 8nm, to be zero.

Computer simulation results for stoichiometry curves with several interaction strengths and $K_2 = 10$ are shown in Figure 5b. It is important to note that the interaction changes the form of the stoichiometry curves. At fixed concentration the attraction between bound dimers always results in a higher stoichiometry. The plateau with stoichiometry close to one head per binding site becomes broadened. If the interaction is stronger than its critical value, one can see the remnant of a phase transition. At a certain concentration there is a sharp step in the stoichiometry, which is somewhat smeared due to finite-size effects. The presence of such a phase transition explains the observed phase segregation at low kinesin concentrations. In the following we will estimate the interaction strength necessary for the existence of the phase transition and the solution concentration at which it occurs.

(b) Coexistence of empty and decorated microtubules

The observation that empty and decorated microtubules can coexist beside each other implies that there is a phase transition between the empty and the decorated phase, akin to the liquid-vapour transition of a fluid. In this analogy, the pressure would correspond to the kinesin concentration in solution and the density to the stoichiometry of bound kinesin heads. At temperatures below the critical point, the liquid and the gaseous phase will coexist in a vessel if the volume lies within a certain range. The phase transition is a clear consequence of an attractive interaction between the molecules. The same is true for phase transitions on surfaces, except that we deal with a two-dimensional model. Such models, known as lattice gas models, have been widely used to describe the adsorption of atoms on crystal surfaces. Fig. 6 shows two snapshots of a simulation on a system of 4 microtubules with a substoichiometric kinesin concentration and two different values of the interaction potential J . If the interaction is strong enough, the simulation shows coexisting empty and decorated microtubules. The decorated state also shows a two-dimensional crystalline structure with 16nm longitudinal periodicity. In the following, we will use a simplified model to explain this behavior and estimate the critical value of the interaction potential.

To keep the model transparent, we will restrict ourselves to the limit $K_2 \gg 1$ in what follows. This simplification implies that it is very unlikely to find a dimer in a state with only one head attached. If there were no interaction with the neighbors, the ratio of transition rates between an empty and an occupied state would be $K_1 K_2 c$, where c is the solution concentration. The chemical potential of the bound molecules is $\mu = k_B T \ln(K_1 K_2 c)$. Two molecules on nearest neighbor sites attract themselves with a binding potential J . The probability to find the lattice in a given state is then proportional to

$$P_{\{n\}} \propto \exp \left[- \sum_{x,y} \left(-J_L n_{x,y} n_{x+2,y} - J_T n_{x,y} n_{x,y+1} - \mu n_{x,y} \right) / k_B T \right], \quad (12)$$

where the coordinates (x,y) run over all lattice sites. The occupation number $n_{x,y}$ is 1 if the two heads of a dimer occupy the binding sites (x,y) and $(x+1,y)$ and is 0 otherwise. Since each binding site can be occupied with at most one head, $n_{x,y}$ and $n_{x+1,y}$ cannot have the value 1 at the same time.

To determine the critical point, we make a further simplification and assume a 16nm longitudinal periodicity meaning that all dimers bind on sites with even x coordinates. This assumption is certainly valid for strong interaction where we have a sharp transition from the empty to the

decorated state with 16nm periodicity.

Then our model simplifies to a conventional lattice gas with nearest-neighbor interaction, which can be mapped onto a 2D Ising model³⁹ for a ferromagnet, whose critical point has been determined exactly by Kramers and Wannier⁴⁰. It is determined by the following condition

$$\sinh \frac{J_L}{2k_B T} \cdot \sinh \frac{J_T}{2k_B T} = 1. \quad (13)$$

For an isotropic interaction, $J_L=J_T=J$, this gives the critical interaction

$$J_c = 1.76 k_B T. \quad (14)$$

This result indicates that the attraction between adsorbed molecules has to be at least J_c in order to allow for a phase transition.

Calculating the full form of the binding stoichiometry as a function of concentration, however, would be equivalent to calculating the magnetization of the two-dimensional Ising model in the presence of an external field, which has not yet been done analytically. Therefore one has to rely on computer simulations to obtain the stoichiometry curves. An overview on Monte-Carlo simulations on lattice gas models has been given by Binder & Landau⁴¹. The situation simplifies when one is far away from the critical point, i.e. when the coupling is much stronger than its critical value, $J \gg J_c$. This corresponds to the low-temperature limit in the Ising analogue. There the stoichiometry reads

$$v = \Theta(\mu + J_L + J_T) \quad (15)$$

where $\Theta(x)$ has the value 1 for $x > 0$ and 0 for $x < 0$. This expression can also easily be understood directly. We obtain full decoration if a dimer in a corner element of a decorated domain (having two bound neighbors) is stable and an empty lattice otherwise. Deviations from Equation (15) can occur due to the finite size of the tubulin plates. The finite-size effect always lowers the number of bound molecules compared to the model on an infinite lattice.

The presence of a phase transition explains why decorated and empty microtubules can coexist beside each other (Fig. 1b). Note that coexistence of empty and decorated microtubules is only possible in a finite system when one takes into account that the solution concentration decreases when some kinesin gets bound. If c_{tot} denotes the total kinesin concentration and c_{tubulin} the total tubulin concentration, then the actual kinesin concentration in solution is given as $c = c_{\text{tot}} - v c_{\text{tubulin}}$.

Now one might ask why the coexistence of empty and decorated microtubules has only been observed with dimeric, but not with monomeric kinesin. A straightforward explanation is that the interaction constants J_L and J_T are smaller for monomers than for dimers and therefore below their critical value which would allow a phase transition. There are at least three possible origins for the smaller interaction strength among monomers. First, if the interaction acts directly between the heads one expects the lateral interaction between two monomers to be only half as strong as between two dimers (Fig. 5a). Second, if the interaction is mediated by structural distortions in the tubulin lattice, it may be much weaker in the case of monomers than in the case of dimers since only a dimer is capable of significantly tilting the underlying tubulin units. And third, the interaction could be mediated by the coiled-coil domain which is missing in monomers.

(c) Two-dimensional crystalline ordering (single-site nucleation vs. annealing)

Thus far we have been describing the equilibrium state of homogeneous, defect-free decoration of microtubules by kinesin. We have shown that with sufficient interaction strength, the equilibrium state is either an empty microtubule (at low concentrations of kinesin) or a microtubule decorated with a two-dimensional periodic kinesin lattice. Now we ask what the dynamic processes which lead to the final equilibrium state are. Starting with an empty microtubule template we can distinguish two pathways of attaining the equilibrium state, nucleation at a single site, or initial

binding at multiple sites followed by annealing (Fig. 7).

Before the decoration starts, the microtubules are always in the empty state. Upon adding kinesin its concentration increases rapidly to the value c and the empty state becomes metastable. The transition to the stable state in which the microtubules are almost entirely decorated can be propagated only after a cluster of kinesin molecules has adsorbed to the microtubule surface in a defined microcrystalline order and has reached a critical size. This process is called *nucleation*. If the decorated area grows by extension of a single nucleus, it can form a regular lattice along the entire microtubule with 16nm longitudinal periodicity. Single-site nucleation can thus provide an explanation for a homogeneous decoration over the whole microtubule, reached in a comparatively short time. The process is akin to the nucleation in the surface adsorption of gas molecules on metal surfaces which has been studied extensively⁴².

Alternatively, the equilibrium state can be reached through an annealing process, where the decoration of the microtubule surface starts at many sites in parallel. This will generate many locally ordered areas which may be out of phase on the 16nm lattice. In order to finally reach a homogeneous decoration with only one predominant domain a secondary process is needed which leads to a coarsening of the initial grainlike structure. This secondary process includes domain wall wandering and annihilation induced by the detachment and re-attachment of kinesin dimers. Typically, however, one expects that such an annealing process will take a very long time. Hence, this pathway of achieving a homogeneous decoration will be very inefficient.

The criterion to recognize which mechanism leads to the ordered state can be stated as follows. If the nucleation time, (the average time needed before a nucleus appears) is longer than the time a nucleus needs to spread over the surface, there is a high chance that the entire surface will be decorated from one nucleus and thus homogeneously. On the other hand, if a second nucleus appears before the first one is able to cover the surface, they may be out of phase (shifted by 8nm) and thus a domain wall appears between them. In this case annealing is necessary to obtain the ordered state, which takes a long time. An analytical expression for the nucleation time can be given if the interaction is strong enough, and the critical cluster size becomes as small as 4, 3 or 2 molecules⁴³. For larger critical cluster sizes, only rough estimates can be given analytically. For example, it has been found that the nucleation rate depends on a kinesin concentration to a power which is typically half the number of nucleus-forming units⁴⁴. However, we are mainly interested in giving a lower limit on interaction necessary to obtain a defect-free decoration, so that the nucleating clusters under consideration are larger. Therefore we use a computer simulation to determine parameter ranges for homogeneous and for inhomogeneous decoration. Homogeneous decoration is reached quickly through the process of single-site nucleation in a sliver close to the transition between the decorated and empty lattice (Fig. 8). In a realistic situation the total kinesin concentration might be of the same order of magnitude as the concentration of tubulin binding sites. Then the kinesin concentration in solution drops as some of the kinesin gets bound. For example, if we are dealing with an initial 2-fold excess of kinesin over microtubule binding sites, the concentration will drop to about half of its initial value. Therefore we estimate that the single-site nucleation has to be dominant at concentrations twice as high as at the phase transition. From Fig. 8 we therefore estimate the interaction needed to obtain monocrystalline ordering by single-site nucleation as $J \approx 3k_b T$. A further important implication of our model is that defect-free decoration is most probable at concentrations just above the phase transition (the threshold for decoration).

Nucleation is also essential for the occurrence of coexisting empty and decorated domains at sub-stoichiometric concentrations. If the nucleation is faster than the growth of the nuclei (multiple-site nucleation), the decoration will start at many microtubules in parallel. After some time, as an increasing amount of kinesin gets bound, its concentration in the solution drops and the growth of decorated domains slows down until some equilibrium concentration is reached. After this initial phase, decorated domains are distributed over all microtubules. Then the smaller domains will

shrink on average while the bigger ones will grow, until the state with segregated phases is reached after some long time. On the other hand, single-site nucleation leads to the occurrence of coexisting empty and decorated microtubules immediately. When a nucleus appears on one microtubule, it quickly covers its surface. This process can repeat on other microtubules until the concentration drops below the value at which the nucleation is possible.

DISCUSSION

In this study we have considered the dynamics and cooperativity of the decoration of microtubules by motor proteins such as kinesin or NCD. We have presented a theory quantitatively describing three major findings of decoration experiments with kinesin dimers:

1. binding stoichiometries between 1 and 2 heads per binding site depending on two binding constants and the kinesin concentration,
2. observed two-dimensional ordering of bound kinesin molecules with 16nm longitudinal periodicity, and
3. coexistence of empty and decorated microtubules in the same solution as a consequence of the attractive interaction between dimers.

While the first two points are based on previously existing experimental observations, we have also presented new experimental data supporting point 3.

All these findings are characteristic for dimeric motors. For *monomeric head domains* (i.e. truncated motors that lack the coiled-coil interaction domain) we find that they bind to microtubules according to a simple lattice-ligand model (Fig. 2a). Each head binds independently since it is small compared with the lattice spacing (8 x 5 nm) so that they can bind independently of each other. As a result, neither crowding nor cooperative phenomena occur. We note that cooperative effects could still occur if there was an interaction between neighboring bound motors; however, there is no experimental evidence to support such an assumption.

For *dimeric motor domains* the situation becomes much more complex. The individual heads are no longer independent, crowding on the microtubule surface has to be considered, and adjacent motors could interact, leading to cooperative effects. We have first discussed a model without explicit attractive interaction between bound dimers and derived an analytical expression for the overall binding stoichiometry of two-headed motors in equilibrium. It depends on the kinesin concentration and two binding constants, K_1 and K_2 , for the first and second head, respectively. The concentration dependence differs qualitatively from that of monomeric motor domains. Whereas for monomeric domains the stoichiometry rapidly grows from 0 to 1, it will finally approach 2 for dimeric constructs if the solution concentration becomes high enough. But most importantly, there is an intermediate plateau regime with a stoichiometry close to 1 if the binding constant of the second head is much larger than 1. The stoichiometry at the largest experimentally accessible concentrations can take values between 1 and 2 motor heads per microtubule subunit, in agreement with recent experiments^{28,20}. This explains why different motors like kinesin and NCD can have different preferred stoichiometries, depending on the relative strength of the interactions between the two motor domains, or between a motor domain and the microtubule (Fig. 4). Thus, under standard decoration conditions, kinesin tends to show stoichiometries around 1 (both heads bound to different tubulin subunits), whereas NCD tends to show stoichiometries around 2 (only one head bound directly, the second tethered loosely). The stoichiometry can also depend on the nucleotide state (ADP, AMP-PNP, etc.). However, the important point is that there is a continuum of possibilities which is both concentration- and time-dependent. Information contained in this dependence may even reveal additional features of the interaction between motor domains and molecular tracks. One of the consequences is that image reconstructions cannot simply be

interpreted in terms of idealized stoichiometries; this likely explains much of the existing controversies (reviewed by Mandelkow and Hoenger²³).

A second feature emerging from our model is that of cooperativity between motors on the microtubule surface. Experimentally, evidence for cooperativity comes in two forms: (i) the coexistence of fully decorated microtubules and bare microtubules (Fig. 1b), (ii) the axial super-periodicity of 16 nm (twice the spacing of tubulin heterodimers) along microtubules (Fig. 1a, cf. Thormählen et al.²⁸).

The all-or-nothing decoration effect can be explained by a nucleation period where a kinesin lattice must first become initiated and stabilized before it expands on the microtubule lattice. If the nucleation barrier is high, only few nucleation sites will form which can then spread quickly and cover an entire microtubule, leaving others in the neighborhood bare. This effect is akin to the well studied nucleation of gas molecules on a metal lattice⁴². It is observed preferentially at low kinesin concentrations where the nucleation barrier is most obvious (because nucleation depends on a higher power of kinesin concentration, typically half the number of nucleus-forming units⁴⁴). A very similar behavior has been observed for the binding of dimeric myosin molecules (HMM) on filaments of F-actin³⁰.

The occurrence of 16 nm periodicity depends on two conditions. First, there has to be a preferred interaction between kinesin dimers on the microtubules, such that neighboring motor molecules are aligned along the 3-start helix of microtubules. The motor heads themselves are spaced 8 nm apart, but the connecting neck domains are 16 nm apart. If the microtubule surface were decorated by random attachment of motor heads, the 16 nm periodicity would be laterally averaged out, and there would be local over-decoration (i.e. 2 heads per tubulin subunit) and under-decoration (holes). Lateral alignment of kinesin dimers can come about only if one assumes some energetically preferred interaction, either between neighboring kinesin dimers themselves (as shown in Fig. 5), or possibly mediated through the tubulin lattice. Second, the nucleation has to take place on a single or on a few sites. Otherwise one would obtain a separate domain for each nucleation site. These domains would locally contain an ordered structure. However, two neighboring domains could be out of phase (shifted by 8 nm) and the 16 nm periodicity would be averaged out to a large extent. A Java applet showing the nucleation process with parameter sets for single-site and multi-site nucleation with subsequent slow annealing can be viewed at <http://www.ph.tum.de/~avilfan/decor/>.

Both findings of the two-dimensional ordering and the coexistence of empty and decorated microtubules clearly indicate an attractive interaction between attached dimers. Equally interesting is the fact that there is no evidence for such an interaction between bound kinesin monomers. This allows three possible explanations:

1. If the interaction acts directly between the heads one expects the lateral interaction between two monomers to be only half as strong as between two dimers (Fig. 5a). Therefore the interaction between monomers might not be strong enough to reach the critical point and no cooperative phenomena are observed.
2. If the interaction is mediated by the coiled-coil domain it is naturally missing in monomers.
3. If the interaction is mediated by structural distortions in the tubulin lattice, it might be much weaker between monomers than between dimers since a dimer can cause significantly stronger structural distortions in underlying tubulin units. A possible hint may be provided by the behavior of a mutant kinesin rK379-A339C which seems to impose a strain on the microtubule lattice resulting in the release of long decorated protofilaments. If such a strain was a characteristic of hand-over-hand binding of kinesin, naturally it would be lacking in monomeric constructs.

Since the two-dimensional ordering is observed on microtubules much less often than on tubulin sheets, we also expect that the cooperativity is stronger on sheets. This observation, too, is

consistent with all three possible origins of the attractive interaction. If the interaction is mediated by direct contact between kinesin heads or their coiled-coil domains, it is obvious that the lateral interaction be smaller on microtubules where the heads are farther apart from each other due to the surface curvature. On the other hand, if the interaction is mediated by structural distortions in the tubulin, it might as well be weaker on tubes since they have a higher mechanical stability.

Hence, if there is an attractive interaction between kinesins on microtubules, which consequences does it have for the function of kinesin *in vivo*? It cannot be a major component of the kinesin motility mechanism since single kinesin dimers have been shown to move along microtubules³. However, in the transport of a vesicle or an organelle many motors are involved at the same time and although they do not reach the densities as used in decoration experiments, they can be close enough for the interaction to become important. A possible function of the interaction would then be to synchronize running motors in order to prevent “traffic jams” on “microtubule highways”.

In summary, we have presented a model explaining the dynamics and cooperativity of the decoration of microtubules with motor proteins. The results show that the interaction between microtubules and different types of motors (kinesin, NCD) can be explained by a dimer adsorption model with different binding affinities. The observed configuration additionally depends on nearest neighbor interactions and the type of nucleation processes. An immediate consequence is that the results from image reconstructions cannot be interpreted by assuming simple binding stoichiometries, as has been done in the past. More generally, the model opens approaches for testing the interactions of motors on microtubules. This will become important when considering the interaction of small clusters of motors, bound to, say, large organelles such as mitochondria. Likewise, the model will be adaptable to other analogous systems, such as the interaction of myosin motors with actin filaments.

MATERIALS AND METHODS

(a) Cloning and protein preparation:

Tubulin was prepared by phosphocellulose chromatography preceded by a MAP-depleting step as described⁴⁵. Microtubules were polymerized in reassembly buffer (0.1 M PIPES, pH 6.9, 1 mM MgCl₂, 0.5 mM EGTA, 1 mM DTT) with 50 μM taxol and 1 mM GTP from a solution containing 15 mg/ml of PC-tubulin on incubation at 37°C for 20 min.

The cloning of the squid kinesin construct sqK498 (containing the motor domain and part of the stalk) was described in a previous publication²⁸. Plasmid sqK338 (containing the motor domain only) was cloned by insertion of an oligonucleotide containing a STOP codon. The plasmid coding for rat kinesin construct rK379 was cloned as described earlier¹⁶. The recombinant kinesin heavy chain fragments were expressed in *E. coli* BL21 (DE3) cells, in the case of sqK498 in the presence of elevated levels of bacterial GroEL/ GroES²⁸.

E. coli cells were grown in LB medium. Expression of kinesin and overexpression of GroEL and GroES protein was induced with 0.4 mM IPTG at a cell density corresponding to A₆₀₀ = 0.6-0.8. Cells were harvested after 16 hours of induction at 25°C, resuspended in lysis buffer (50 mM PIPES, pH 6.9, 60 mM NaCl, 1 mM MgCl₂, 0.5 mM EGTA, 2 mM DTT, 1mM PMSF) and lysed with a French press. Further purification was done either by affinity purification on microtubules followed by ion exchange chromatography on a MonoQ column (sqK338, sqK498) as described previously³¹, or by ion exchange chromatography on phosphocellulose and MonoQ (rK379).

(b) Electron microscopy:

Microtubules were prepared as described above. To obtain full decoration microtubules were

diluted to 0.2 mg/ml (2 μ M tubulin dimers) into RB buffer containing 10 μ M taxol, 1 mM AMPPNP and a 3 to 5 fold molar excess (i.e., 6 – 10 μ M) of kinesin heads and incubated at room temperature. After 10 minutes the decorated microtubules were spun down in a Beckman TL 100 ultracentrifuge, the supernatant was removed and the microtubules were resuspended in RB buffer supplemented with 1 mM AMPPNP/10 μ M taxol. This procedure was repeated at least once, before a drop of the sample was applied to a carbon coated EM grid and stained with a solution of 1% uranyl acetate. Decoration with sqK338 by the method described above led to microtubule bundling. Here, microtubules were first allowed to adsorb to the carbon surface before the grid was placed in a drop of sqK338 solution at 0.5 mg/ml protein and 1 mM AMP-PNP. After 5 min at room temperature the sample was washed by transferring the grid to several drops of buffer (RB with 1 mM AMPPNP/10 μ M taxol) and finally stained. Specimens showing partial decoration were obtained by the standard procedure described above except that the molar ratio of kinesin heads to tubulin dimers was only 1 : 1, or lower. Mixing effects can be excluded because a small volume of microtubules was mixed with a larger volume of kinesin-containing solution and the probability of encountering a kinesin molecule was roughly equivalent for each microtubule. Electron microscopy was performed using a Philips CM12.

(c) Computer modeling of microtubule decoration by kinesin:

Simulations were performed on a rectangular lattice of 100 (length) times 14 (width) binding sites. We started each simulation with an empty lattice. Then the mean dwell time in a certain state was obtained as the inverse of the sum of all reaction rates. The step time was then chosen randomly with an exponential distribution and the average given by the dwell time. The configuration in the next simulation step was determined by randomly choosing one of the possible reactions with probability proportional to its rate.

For studying the effects of nucleation and annealing of the kinesin lattice on the microtubule surface, we restricted ourselves to the limit $K_2 = 0$ as described in Results, Sect. 3b, thus reducing the number of parameters. We used the same simulation algorithm, and ran the simulation until 90% of the lattice was filled. Each simulation was repeated 100 times and those runs leading to at least 95% in-phase decoration were counted as being homogeneous. Finally the line where the fraction of runs with homogeneous decoration reaches 50% was computed and plotted in Fig. 8.

All other theoretical considerations are described in Results, sections 2 and 3. A Java applet visualizing the computer simulation of microtubule decoration can be viewed on the internet at <http://www.ph.tum.de/~avilfan/decor/>.

Acknowledgements: This work has been supported by the Deutsche Forschungsgemeinschaft under Grant SPP 1068, Grant SFB 413 (A.V., E.F. and F.S.) and a Heisenberg fellowship (FR 850/3) (E.F.).

References

1. Howard, J. (1997). Molecular motors: structural adaptations to cellular functions. *Nature*, **389**, 561-567
2. Hancock, W.O. & Howard, J. (1998). Processivity of the motor protein kinesin requires two heads. *J. Cell. Biol.*, **140**, 1395-1405
3. Svoboda, K., Schmidt, C.F., Schnapp, B.J. & Block, S.M. (1993). Direct observation of kinesin stepping by optical trapping interferometry. *Nature*, **365**, 721-727
4. Visscher, K., Schnitzer, M.J. and Block, S.M. (1999). Single kinesin molecules studied with a molecular force clamp. *Nature*, **400**, 184-189
5. Inoue, Y., Toyoshima, Y., Iwane, A., Morimoto, S., Higuchi, H. & Yanagida, T. (1997). Movements of truncated kinesin fragments with a short or an artificial flexible neck. *Proc. Natl. Acad. Sci. USA*, **94**, 7275-7280
6. Romberg, L., Pierce, D. & Vale, R.D. (1998). Role of the kinesin neck region in processive microtubule-based motility. *J. Cell Biol.*, **140**, 1407-1416
7. Hirose, K., Lockhart, A., Cross, R.A. & Amos, L.A. (1996). Three-dimensional cryoelectron microscopy of dimeric kinesin and *ncd* motor domains on microtubules. *Proc. Natl. Acad. Sci. USA*, **93**, 9539-9544
8. Hirose, K., Löwe, J., Alonso, M., Cross, R.A. & Amos, L.A. (1999). Congruent docking of dimeric kinesin and *ncd* into three-dimensional electron cryomicroscopy maps of microtubule-motor ADP complexes. *Mol. Biol. Cell*, **10**, 2063-2074
9. Arnal, I., Metoz, F., DeBonis, S. & Wade, R.H. (1996). Three-dimensional structure of functional motor proteins on microtubules. *Current Biology*, **6**, 1265-1270
10. Hoenger, A., Sablin, E.P., Vale, R.D., Fletterick, R.J. & Milligan, R.A. (1995). Three-dimensional structure of a tubulin-motor-protein complex. *Nature*, **376**, 271-274
11. Hoenger, A., Sack, S., Thormählen, M., Marx, A., Müller, J., Gross, H. & Mandelkow, E. (1998). Image reconstruction of microtubules decorated with monomeric and dimeric kinesin: Comparison with x-ray structure and implications for motility. *J. Cell Biol.*, **141**, 419-430
12. Sosa, H., Dias, D.P., Hoenger, A., Whittaker, M., Wilson-Kubalek, E., Sablin, E., Fletterick, R.J., Vale, R.D. & Milligan, R.A. (1997). A model for the microtubule-*Ncd* motor protein complex obtained by cryo-electron microscopy and image analysis. *Cell*, **90**, 217-224
13. Kull, F.J., Sablin, E., Lau, P., Fletterick, R. & Vale, R. (1996). Crystal structure of the kinesin motor domain reveals a structural similarity to myosin. *Nature*, **380**, 550-554
14. Sablin, E.P., Kull, F.J., Cooke, R., Vale, R.D. & Fletterick, R.J. (1996). Crystal structure of the motor domain of the kinesin-related motor *ncd*. *Nature*, **380**, 555-559
15. Sack, S., Müller, J., Marx, A., Thormählen, M., Mandelkow, E.-M., Brady, S.T. & Mandelkow, E. (1997). X-ray structure of motor and neck domain from rat brain kinesin. *Biochemistry*, **36**, 16155-16165
16. Kozielski, F., Sack, S., Marx, A., Thormählen, M., Schönbrunn, E., Biou, V., Thompson, A., Mandelkow, E.-M. & Mandelkow, E. (1997). The crystal structure of dimeric kinesin and implications for microtubule-dependent motility. *Cell*, **91**, 985-994
17. Sablin, E.P., Case, R.B., Dai, S.C., Hart, C.L., Ruby, A., Vale, R.D. & Fletterick, R.J. (1998). Direction determination in the minus-end-directed kinesin motor *ncd*. *Nature*, **395**, 813-816
18. Nogales, E., Wolf, S. & Downing, K. (1998). Structure of the $\alpha\beta$ tubulin dimer by electron crystallography. *Nature*, **391**, 199-203
19. Nogales, E., Whittaker, M., Milligan, R.A. & Downing, K.H. (1999). High resolution model of the microtubule. *Cell*, **96**, 79-88
20. Hoenger, A., Thormählen, M., Diaz-Avalos, R., Doerhoefer, M., Goldie, K.N., Müller, J. & Mandelkow, E. (2000). A new look at the microtubule binding patterns of dimeric kinesins. *J. Mol. Biol.*, **279**, 1087-1103
21. Kikkawa, M., Okada, Y. & Hirokawa, N. (2000). 15 angstrom resolution model of the monomeric kinesin motor. *Cell*, **100**, 241-252
22. Kawaguchi, K. & Ishiwata, S. (2001). Nucleotide-dependent single- to double headed binding of kinesin. *Science*, **291**, 667-669
23. Mandelkow, E. & Hoenger, A. (1999). Structures of kinesin and kinesin-microtubule interactions. *Curr. Opin. Cell Biol.*, **11**, 34-44
24. Hirokawa N. (1998). Kinesin and dynein superfamily proteins and the mechanism of organelle transport. *Science*, **279**, 519-526
25. Goldstein, L.S.B. & Philp, A.V. (1999). The road less traveled: Emerging principles of kinesin motor utilization. *Annu. Rev. Cell Dev. Biol.*, **15**, 141-183
26. Hackney, D.D. (1994). Evidence for alternating head catalysis by kinesin during microtubule-stimulated ATP hydrolysis. *Proc. Nat. Acad. Sci. USA*, **91**, 6865-6869
27. Sack, S., Kull, J.F. & Mandelkow, E. (1999). Motor proteins of the kinesin family – Structures, variations, and nucleotide binding sites. *Eur. J. Biochem.*, **262**, 1-11
28. Thormählen, M., Marx, A., Müller, S.A., Song, Y.-H., Mandelkow, E.-M., Aebi, U. & Mandelkow, E. (1998). Interaction of monomeric and dimeric kinesin with microtubules. *J. Mol. Biol.*, **275**, 795-809

29. Lockhart, A., Crevel, I.M. & Cross, R.A. (1995). Kinesin and ncd bind through a single head to microtubules and compete for a shared MT binding site. *J. Mol. Biol.*, **249**, 763-771
30. Orlova, A. & Egelman, E. (1997). Cooperative rigor binding of myosin to actin is a function of F-actin structure. *J. Mol. Biol.*, **265**, 469-474
31. Song, Y.H. & Mandelkow, E. (1993). Recombinant kinesin motor domain binds to β -tubulin and decorates microtubules with a B-surface lattice. *Proc. Natl. Acad. Sci. USA*, **90**, 1671-1675.
32. Thormählen, M., Marx, A., Sack, S. & Mandelkow, E. (1998). The coiled-coil helix in the neck of kinesin. *J. Struct. Biol.*, **122**, 30-41
33. Ma, Y.-Z. & Taylor, E.W. (1995). Kinetic mechanism of kinesin motor domain. *Biochemistry*, **34**, 13233-13241
34. Moyer, M.L, Gilbert, S.A. & Johnson, K.A. (1998). Pathway of ATP hydrolysis by monomeric and dimeric kinesin. *Biochemistry*, **37**, 800-813
35. Mandelkow, E. & Johnson, K.A. (1998). The structural and mechanochemical cycle of kinesin. *Trends Biochem. Sci.*, **23**, 4229-433
36. Hancock, W.O. & Howard, J. (1999). Kinesin's processivity results from mechanical and chemical coordination between the ATP hydrolysis cycles of the two motor domains. *Proc. Natl. Acad. Sci. USA*, **96**, 13147-13152
37. McGhee, J.D. & von Hippel, P.H. (1974). Theoretical aspects of DNA-protein interactions: Co-operative and non-co-operative binding of large ligands to a one-dimensional homogeneous lattice. *J. Mol. Biol.*, **86**, 469-489
38. Hill, T.L. (1985). Cooperativity Theory in Biochemistry. Springer, New York
39. Yeomans, J.M. (1992). Statistical mechanics of phase transitions. Clarendon Press, Oxford
40. Kramers, H.A. & Wannier, G.H. (1941). Statistics of the two-dimensional ferromagnet. Part I. *Phys. Rev.*, **60**, 252-276
41. Binder, K. & Landau, D.P. (1989). Monte Carlo calculations on phase transitions in adsorbed layers. *Adv. Chem. Phys.*, **76**, 91-152
42. Lewis, B. & Anderson, J.C. (1978). Nucleation and Growth of Thin Films, Chapter 4. Academic Press, London
43. Becker, R. & Döring, W. (1935). Kinetische Behandlung der Keimbildung in übersättigten Dämpfen. *Annalen der Physik (V)*, **24**, 719-752
44. Oosawa, F. & Asakura, S. (1975). Thermodynamics of the polymerisation of protein. Academic Press, London
45. Mandelkow, E.M. & Mandelkow, E. (1985). Unstrained microtubules studied by cryo-electron microscopy: substructure, supertwist and disassembly. *J. Mol. Biol.*, **181**, 123-135

Figures

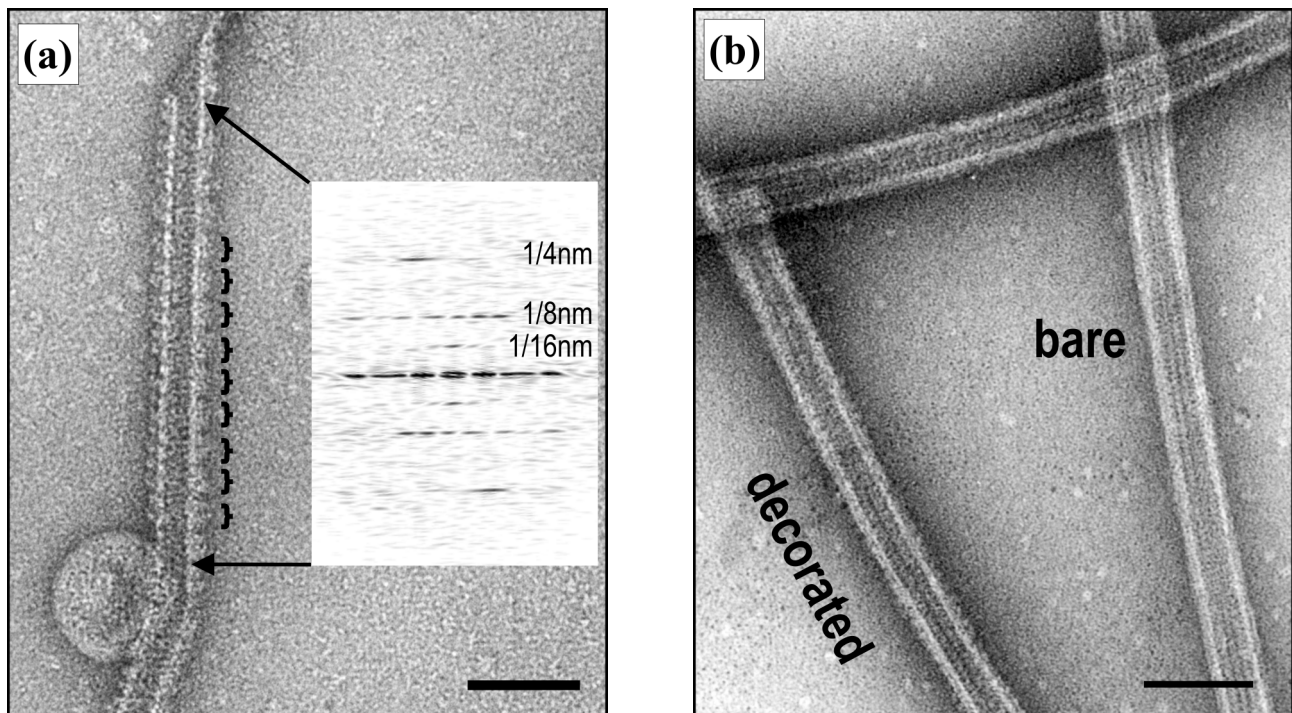


Fig. 1: Electron microscopy (negative staining) of microtubules decorated with kinesin, illustrating normal periodic decoration and cooperative phenomena. Bars = 50 nm.

(a) Microtubule fully decorated with dimeric kinesin heads (sqK498). The structure contains three axial periodicities (see inset), 4 nm (due to tubulin monomers), 8 nm (the spacing of tubulin subunits, enhanced by the binding of kinesin motor domains), and 16 nm (a pairing of kinesin dimers in the axial direction). The specimen is one of several cases where 16 nm periodicities could be observed under routine decoration conditions. However, these periodicities appear to be much less prominent on microtubules than they are on tubulin sheets. In this example they appear as rather diffuse, stain-excluding spots on the right side of the microtubule that have twice the spacing of the kinesin heads on the left side. The inset shows a Fourier calculation of the diffraction pattern of the area indicated by the arrows. The existence of a clear 16 nm periodicity means that kinesin dimers must be aligned in lateral register.

(b) Three microtubules exposed simultaneously to kinesin dimers (rK379) at a low stoichiometric ratio (1 kinesin motor domain per 1 tubulin subunits). Note that two microtubules seem fully decorated while one looks completely empty. This indicates that binding to and filling the microtubule lattice follows a cooperative interaction.

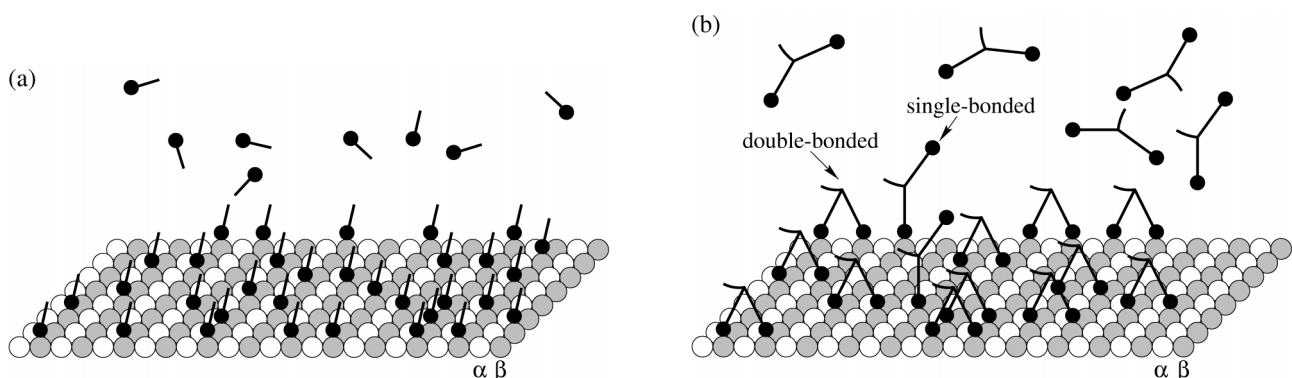


Fig. 2: Schematic representation of the binding of kinesin monomers or dimers to the microtubule surface. The microtubule lattice is shown here as a sheet of 8 protofilaments running in a horizontal direction, with alternating subunits of α -tubulin (white) and β -tubulin (gray); the microtubule plus end is on the right. Kinesin motor domains (heads) are shown as black spheres which bind mainly to β -tubulin. **(a)** Decoration of the microtubule by a monomeric head-linker construct which is too short so that dimerization cannot occur, yet the head is capable of binding to a microtubule. It is assumed that the monomeric heads bind independently of one another, and since the binding sites are far apart compared to the size of the motor domain the crowding does not occur. **(b)** Decoration of the microtubule by a dimeric kinesin construct which is long enough to form a coiled-coil. The dimer can bind to the microtubule either with both heads or with one head only.

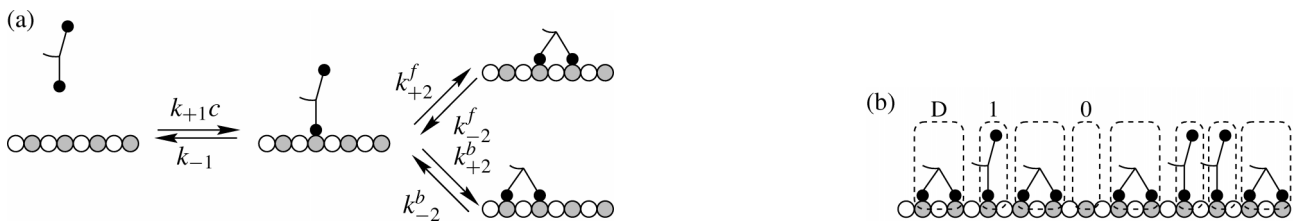


Fig. 3: (a) Reaction rates for association and dissociation of dimeric kinesin assuming freely accessible binding sites on the microtubule lattice. The initial docking of the first head is a second order reaction and depends on the association rate constant k_{+1} and the concentration c of kinesin, all other reactions are first order. Once the first head of a dimer is bound it is assumed that the second head can find a binding position on the next β -tubulin subunit either in the forward direction (towards the plus end, top right, k_{+2}^f) or to in the backward direction (k_{+2}^b).

(b) Configurations of kinesin dimers bound to a protofilament. "D" = dimer with both heads bound to two successive beta-tubulin subunits, "1" = dimer with only one head attached directly ("tightly bound"), the second head connected only via the first one ("loosely bound"). "0" = Empty binding site.

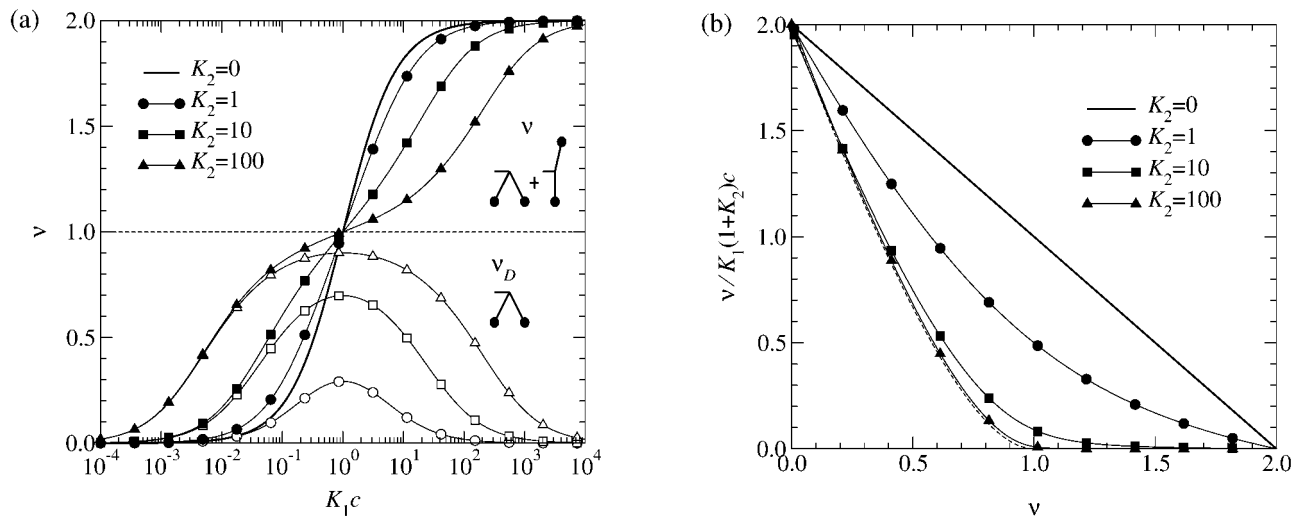


Fig. 4: (a) Binding stoichiometries of dimeric kinesin without attractive interaction between kinesin molecules as a function of the kinesin concentration c for different values of the constant K_2 . The lines with filled symbols indicate the total number of heads per binding site v and those with empty symbols only the number of heads belonging to doubly-attached dimers v_D . Note that when the second head binds strongly (K_2 high) once the first one has docked, it is possible to nearly saturate the microtubule lattice with doubly bound kinesin dimers, yielding a stoichiometry of kinesin heads per tubulin dimer close to $v=1$, provided that the concentration of kinesin is not too large ($K_1c \approx 1$, open triangles). This situation is observed in some image reconstruction studies (e.g. rat kinesin¹¹). At overloading kinesin concentrations (right half of the graph), kinesin dimers attached through only one head become more frequent because at any given free tubulin site, the docking of a new kinesin dimer through its first head is faster than the attachment of the second head of a neighboring kinesin dimer. Eventually the lattice contains almost only singly bound kinesin dimers and almost no doubly bound dimers. This corresponds to an overall stoichiometry of $v=2$ and is experimentally observed with the retrograde motor NCD (one tight, one loosely bound head per kinesin dimer¹²). However, most image reconstructions with kinesin show an intermediate situation with effective stoichiometries around 1.3 - 1.5 (i.e. half the dimers bound through one head only, the other half through both heads).

(b) Same data shown in a Scatchard-plot. A linear curve with a maximum stoichiometry of 2 heads per binding site is obtained for the case where the second head cannot bind ($K_2=0$, top curve). For intermediate cases where singly-bound and doubly-bound kinesin dimers compete the Scatchard plot shows a smooth curvature. At high K_2 , the doubly-bound mode dominates, resulting in a stoichiometry close to 1 (reminiscent of microtubules decorated with rat brain kinesin dimers).

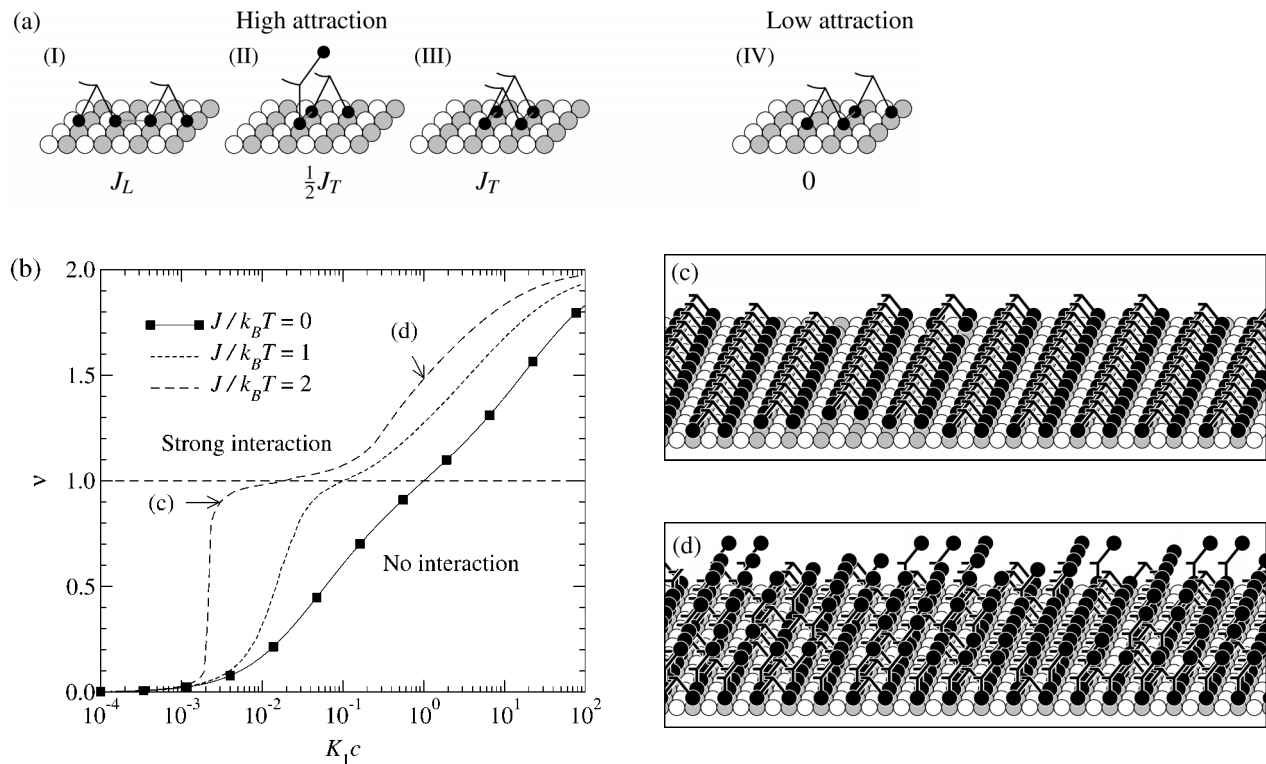


Fig. 5: Model with interaction: (a) The interaction potential between two adsorbed kinesin molecules in different relative positions. (I) We assume a longitudinal attraction with strength J_L between the leading head of one dimer and the trailing head of the next one along the same protofilament. (II) A transverse attraction between two kinesin heads on neighboring protofilaments has the strength $\frac{1}{2}J_T$ if two firmly bound heads are in register and at least one of them belongs to a dimer with the second head loosely bound. (III) The transverse attraction becomes J_T when two adjacent dimers are in register with both firmly attached heads. (IV) However, the interaction becomes 0 when to adjacent kinesin dimers are out of register such that the leading head of one dimer comes to lie next to the trailing head of another. With these assumptions, a binding pattern is favored where kinesin dimers tend to bind in register along the microtubule 3-start helix (as in III). Note that the interactions between the kinesin heads could be either direct, or mediated by the underlying microtubule lattice (e.g. by distortions or conformational changes of the tubulin molecules) (b) Binding stoichiometry (heads per binding site) for three different values of the interaction strength ($J_L=J_T=J=0, 1k_B T$ and $2k_B T$). The binding constant of the second head was chosen as $K_2=10$. The curve for $J=0$ corresponds to the curve for $K_2=10$ in Fig. 4a. The curves were obtained from a computer simulation on a lattice with 100×14 binding sites. (c) A snapshot from the simulation at $K_1 c = 0.003$. Note that a lateral interaction leads to two-dimensional crystalline ordering with 16nm longitudinal periodicity. (d) A snapshot from the simulation at $K_1 c = 1$. The longitudinal periodicity is destroyed since many kinesins are bound with one head only.

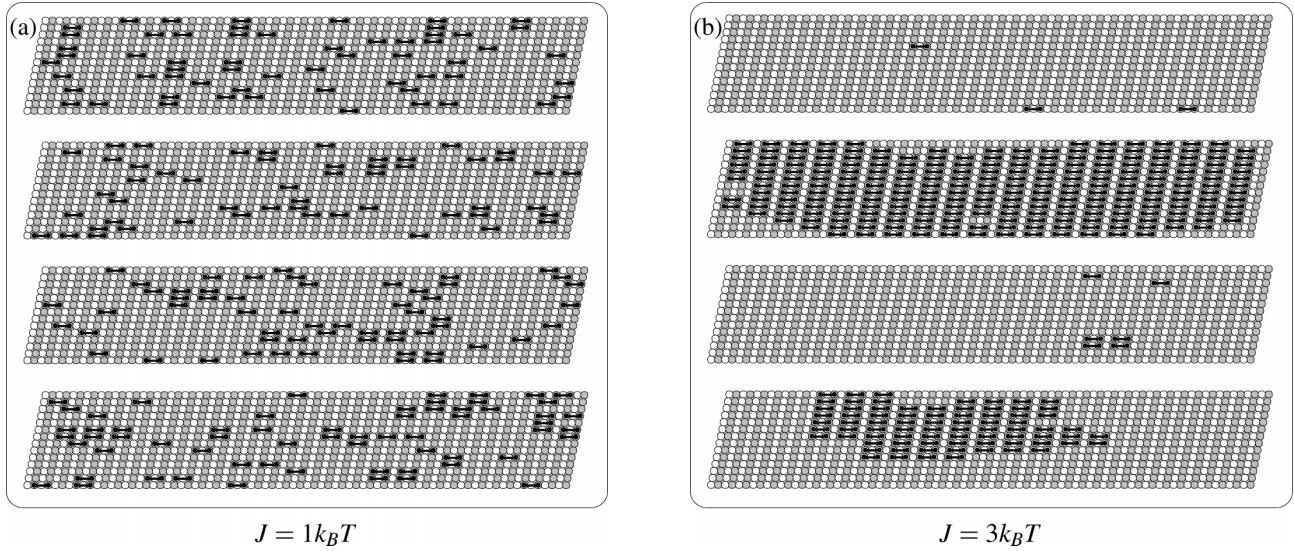


Fig. 6: Coexistence of empty and decorated domains: Typical equilibrium configurations of bound kinesin on microtubules in presence of a weak (a) and strong (b) attractive interaction. Each simulation was performed on a group of 4 separate tubulin sheets. The total kinesin concentration was chosen the way that $c_{tot} = 0.3c_{tubulin}$ and $K_1 K_2 c_{tot} = 1$. The simulation took into account that the concentration of free kinesin decreases as some of it gets bound to microtubules, therefore $c = c_{tot} - \nu c_{tubulin}$. (a) shows a simulation with low interaction strength ($J = k_B T$) and (b) with interaction strength above the critical value ($J = 3k_B T$). In the latter case, the coexistence of empty and decorated microtubules is clearly visible. Kinesin dimers on decorated microtubules form a two-dimensional periodic lattice with 16nm longitudinal periodicity.

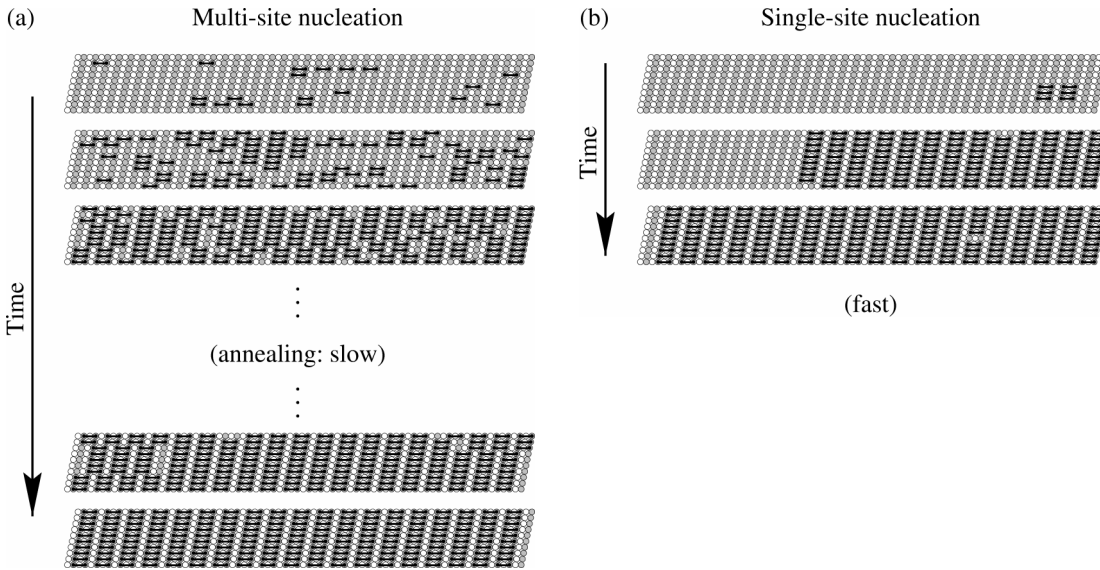


Fig. 7: Nucleation: Computer simulation of multiple-site nucleation with subsequent annealing (a) and single-site nucleation (b). Both can lead to a defect-free decoration. However, annealing can be extremely slow whereas single-site nucleation immediately leads to the ordered state. The parameters in the simulation were the following: (a): $K_1 K_2 c = 0.1$, $A_L = A_T = 3.0$, $B_L = B_T = 0.3$ (b): $K_1 K_2 c = 0.001$, $A_L = A_T = 10.0$, $B_L = B_T = 0.1$.

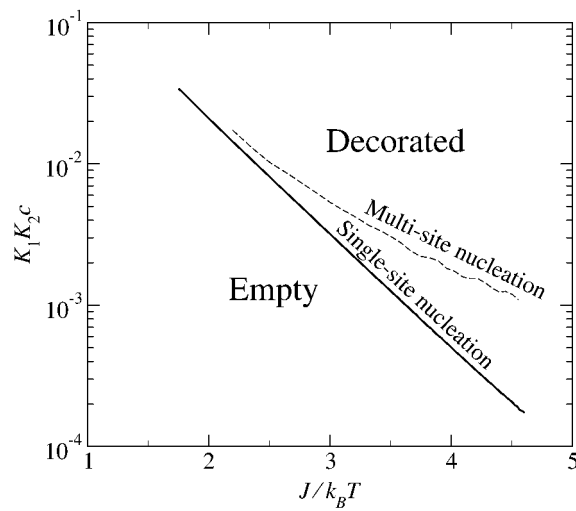


Fig. 8: Phase diagram: The solid line shows the phase transition above which a decorated phase exists. The dashed line shows the border between homogeneous (defect-free) decoration reached immediately through nucleation and decoration with domain walls. The curves were obtained from a computer simulation on a lattice of 14×100 sites (note that the defect-free range would be somewhat larger on a smaller lattice). $J_L = J_T = J$ was assumed. See Materials & Methods for details.